Laser and Particle Beams (2004), *22*, 261–266. Printed in the USA.

DOI: 10.1017/S0263034604223084

Photopumping of XUV lasers by XFEL radiation

KE LAN,[1] ERNST FILL, and JÜRGEN MEYER-TER-VEHN
Max-Planck-Institut für Quantenoptik, D-85748 Garching, Germany

(Received 1 November 2003; Accepted 17 February 2004)

Abstract

Within the next few years X-ray free-electron lasers (XFELs) now under construction are expected to generate highly collimated XUV pulses with 10^{13} photons and a duration of 100 fs. Focusing this radiation to a spot some 10 μm in diameter generates intensities of up to 10^{16} W/cm^2. Such pump intensities make feasible the investigation of photopumped XUV lasers using this radiation. We present simulations taking into account two different mechanisms generating the gain: (1) photoionization with subsequent three-body recombination, which takes advantage of the monochromaticity of the pump radiation to generate very cold electrons; (2) inner-shell ionization in which transient inversion is obtained by generating a hole in an otherwise completely filled shell. The simulations show that under appropriate conditions both mechanisms generate very high gain. However, a number of further issues must be considered, such as the propagation of the pump pulse in the medium to be pumped.

Keywords: Photopumping; X-ray free-electron laser; X-ray laser

1. INTRODUCTION

In recent years significant progress has been achieved in the field of X-ray lasers. Accomplishments include the availability of many laser lines in the soft X-ray region, saturated lasers down to a wavelength of 5 nm, pulses with a duration of a few picoseconds, coherent emission, systematic characterization of many beam parameters, and reduction of the required pump energy to a few joules. In addition, a number of applications have already been realized.

On the other hand, progress in the direction of generating shorter wavelengths has been lacking and the record for the shortest lasing wavelength ever achieved is still held by the Livermore group with the nickel-like gold laser at 3.6 nm (MacGowan *et al.*, 1992). Electron collisional pumping, the most widely used scheme in present-day X-ray laser research (Tallents, 2003), does not scale well to shorter wavelengths.

A possible route toward shorter wavelengths encompasses photopumped lasers because this method scales well in this direction (Elton, 1990). However, in spite of efforts in many laboratories a truly photopumped laser has not been realized so far. One of the reasons for this failure is that a suitable pump source has not been available. Fortunately, this situation will change within a short period of time with the advent of the X-ray free-electron laser (XFEL) at Deutsches Elektronen-SYnchrotron (DESY) Hamburg. This installation will provide not only a source of X-ray photons with high brightness but also the additional features of continuous tunability and a pulse duration in the femtosecond range. This is motivation enough to revisit the photopumping schemes and propose experiments in the direction of a photopumped X-ray laser. New insights into many aspects of atomic, plasma, and laser physics are to be gained in this way, and the experiments may also reveal why previous photopumping experiments failed.

Three different suggestions on how to photopump an X-ray laser have been put forward, namely, *photoionization* pumping, *inner-shell* pumping, and *photoresonant* pumping. In this article we consider only the first two of these because photoresonant pumping can only generate gain between excited energy levels.

The idea of photoionization pumping is to ionize an atom or ion with quasi-monochromatic radiation with a photon energy just above the ionization energy in order to generate very cold electrons (Bunkin *et al.*, 1981; Goodwin & Fill, 1988, 1990). Three-body recombination then proceeds at a high rate, predominantly populating high-lying levels. A subsequent collisional cascade distributes this population among the excited bound levels. If the pump has a sufficiently high intensity, the ground state is fully depleted, and it is possible to generate gain on transitions to that state. In this way gain on He-α or Lyman-α transitions can be achieved and the scheme has a high quantum efficiency.

[1]On leave from the Institute of Applied Physics and Computational Mathematics. P.O. Box 8009-12 Beijing, 100088, China.
Address correspondence and reprint requests to: Ernst Fill, Max-Planck-Institut für Quantenoptik, Hans-Kopfermann-Str. 1, D-85748 Garching, Germany. E-mail: ernst.fill@mpq.mpg.de

We use the parameters of the TESLA Test Facility at DESY/Hamburg (see, e.g., Gerth, 2001; Materlik & Tschentscher, 2001) to investigate the conditions for obtaining gain in a photopumped soft-X-ray laser (Lan *et al.*, 2003). From an experimental point of view the simplest realization of that scheme is to ionize helium (ionization potential 24.6 eV) using a photon energy of, say, 25 eV and look for gain at the He-α transition ($\lambda = 58.4$ nm). Another possibility is the generation of gain on the Lyman-α transition of He II at $\lambda = 30.4$ nm. Simulation of the latter problem is more difficult because the helium gas must first be ionized to the hydrogenic state and then further to bare nuclei. For this purpose a photon energy exceeding that of hydrogenic helium (54.4 eV) is required. The higher photon energy also results in a higher electron temperature because the first ionization produces electrons with a temperature of about 20 eV. Only the second ionization generates very cold electrons and reduces the electron temperature.

A layout of the proposed experiment is shown in Figure 1. The XFEL pump source is weakly focused by a grazing incidence elliptical mirror into a helium gas puff. With an appropriate nozzle, densities exceeding 10^{20} cm^{-3} can be realized. However, it will later be shown that a density of about 10^{19} cm^{-3} is optimal for the particular case of the He-α laser. The generated radiation is dispersed in a transmission grating spectrometer (to separate it from the pump radiation) and detected with a soft-X-ray CCD or by a diode array. A repetition rate of 10 Hz is envisaged for the experiment, making possible adjustments in real time. The requirements for the background pressure in the experimental chamber are not severe, because line broadening and a line shift will prevent the background gas from absorbing the generated XUV lines.

2. SIMULATIONS

Phase II of the TESLA Test Facility installation is projected to emit 10^{13} photons with an energy continuously tunable between 20 eV and 60 eV in a pulse of 100 fs duration. This radiation is well collimated, so that by means of an appropriate mirror, a focus about 10 μm in diameter should be achieved, resulting in intensities exceeding 10^{16} W/cm^2.

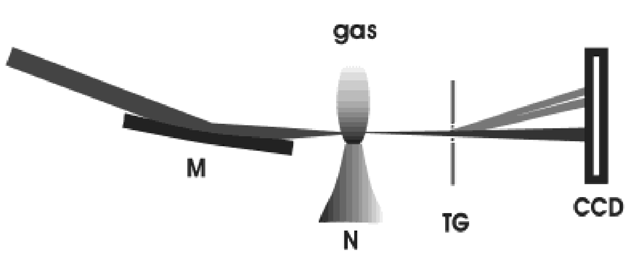

Fig. 1. Experimental setup for XUV laser photopumped by XFEL radiation. XFEL beam is focused into a gas puff generated by the nozzle N by means of grazing incidence mirror M. The emitted radiation is dispersed by a transmission grating TG and detected by means of a CCD.

Due to the short pulse duration the ions remain cold during pumping and for a few hundred femtoseconds thereafter. Ion motion therefore need not be taken into account. However, the high electron density results in a very short electron–electron relaxation time and thus the electrons are assumed to have a Maxwellian velocity distribution. Hydrodynamic motion of the generated plasma is neglected.

The time-dependent occupation of the levels is calculated by means of the CRMHA code (Lan *et al.*, 1999; Lan & Zhang, 2002). In addition to the primary process of photoionization, the code contains the collisional effects of excitation and de-excitation, collisional ionization and three-body recombination. Spontaneous emission and spontaneous and stimulated radiative recombination as well as dielectronic capture are also included. The calculations extend to 500 fs, after which time the basic assumptions of no hydrodynamics and cold ions are expected to be invalidated.

The simulations calculate the electron temperature T_e resulting from photoionization, which is two thirds of the excess energy of the pump photon over the ionization potential. Gain or loss of electron energy due to collisional and radiative processes is taken into account, with the main contribution being due to three-body recombination. Changes in the electron temperature due to radiative processes and inverse Bremsstrahlung are also included

An important issue in calculating the gain is the laser line width. In this work Doppler broadening is neglected owing to the low ion temperature. The dominant contribution to the line width thus comes from Stark broadening. The line widths are taken from Griem (1974). It turns out that for heliumlike ions the quadratic Stark effect leads to a relatively low Stark width. The linear Stark effect in hydrogenic ions generally results, however, in a large width for the hydrogenic lines. The Lyman-α line is still favorable in this respect because for all Lyman lines with even-quantum-number upper levels the line width is reduced.

The simulations start with helium in its ground state at room temperature. At time $t = 0$ a pump pulse with a $\sin^2$ shape and 100 fs FWHM is launched into the medium. For the He-α laser the pump photon energy is taken to be 25 eV, just above the ionization potential of atomic helium of 24.6 eV. For the Lyman-α laser in He II (ionization potential 54.4 eV) a pump photon energy of 55 eV is chosen. Note that the He II laser has ionization of neutral helium well into the continuum. To investigate the sensitivity of the generated gain to any parameter changes the simulations were carried out for a significant range of pump intensities and gas densities. In particular, pump intensities of 10^{13}–10^{16} W/cm^2 were used for He I and 10^{14}–10^{18} W/cm^2 for He II lasing. Gas densities range from 10^{19} to 10^{21} cm^{-3}.

3. SIMULATION RESULTS FOR HE I

This laser operates on the He-α transition of atomic helium with a wavelength of 58.4 nm. Rapid depletion of the helium ground at an intensity of 10^{14} W/cm^2 is illustrated in Fig-

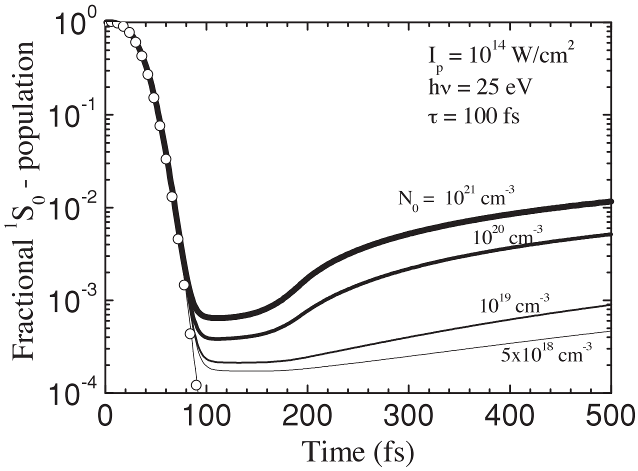

Fig. 2. Temporal evolution of relative ($^1S_0$) ground state population of atomic He for I = 10^{14} W/cm^2 and densities of 5×10^{18}, 10^{19}, 10^{20}, and 10^{21} cm^{-3}. Open circles show the result of a simple theory that takes only photoionization into account.

ure 2. As can be seen, even at the highest density of 10^{21} cm^{-3}, depletion of more than three orders of magnitude is achieved. The open circles show the result of a simple analytical approximation that takes only photoionization (and no recombination) into account. Of course, an empty ground state is of crucial importance for generating gain on the He-α transition and, as will be shown later, for propagation of the pump pulse through the medium. The temporal evolution of the gain on the He-α transition is shown in Figure 3 for different densities N_0. The temporal shape of the pump pulse is also included in the diagram. It is seen that gains of the order of 100 cm^{-1} are generated. The higher the density, the shorter is the duration of the gain. At the lower densities the gain is still rising at the end of the simulation.

It should be kept in mind that generation of a high gain is only a prerequisite for an X-ray laser. Because this laser will be operated as an ASE (amplified stimulated emission) laser even more important is that a high gain length product be achieved. For a gain line dominating the spectrum, a gain length product exceeding about 5 must be achieved; for saturation the gain length product must be 15 or higher. To attain such a high gain length product in a longitudinal pump configuration the pump pulse must be capable of propagating through the medium for a sufficiently long distance. This point is addressed in Figures 4 and 5. In Figure 4 we show contour plots of the intensity of the pump and of the gain for a helium density of 10^{19} cm^{-3} at a pump intensity of 10^{14} W/cm^2. In spite of a high absorption coefficient the pump propagates a distance of >2 mm into the medium. This can be understood by realizing that the helium ground state is strongly depleted, as shown in Figure 2. An interesting feature appears in the gain contour: The gain reaches its highest value only after the pump pulse has propagated about 1 mm into the medium. The reason for this is that the pump pulse steepens upon propagation because the rising

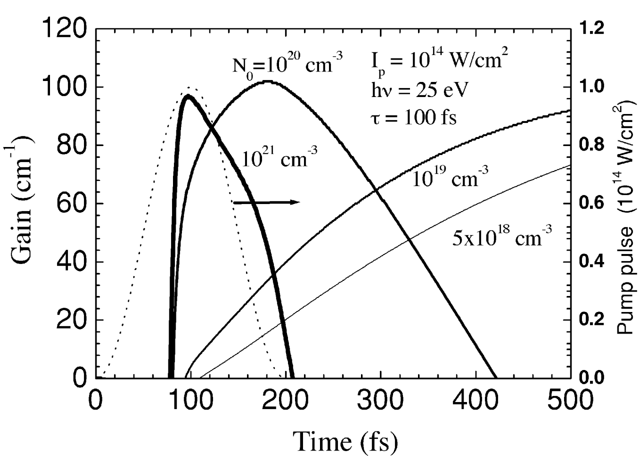

Fig. 3. Temporal evolution of gain for He I laser ($\lambda = 58.4$ nm) at different gas densities. The pump intensity is 10^{14} W/cm^2. The temporal shape of the pump is also shown in the figure.

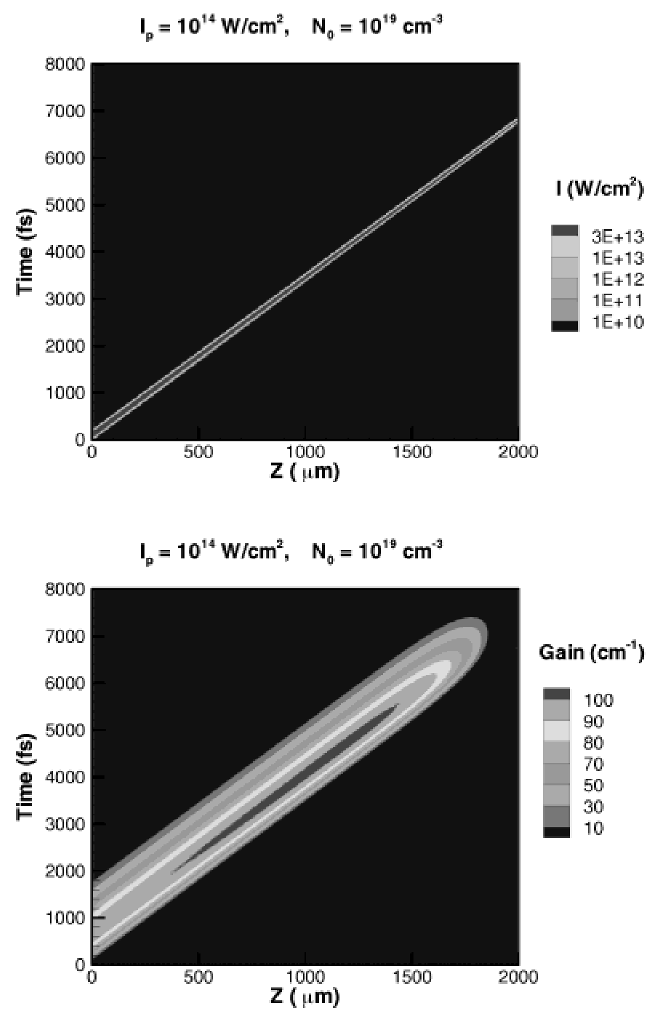

Fig. 4. Contour plot of pump intensity and gain for $N_0 = 10^{19}$ cm^{-3} and $I = 10^{14}$ W/cm^2. The pump pulse is seen to propagate about 2 mm into the medium, generating a gain coefficient of about 100 cm^{-1} over that distance.

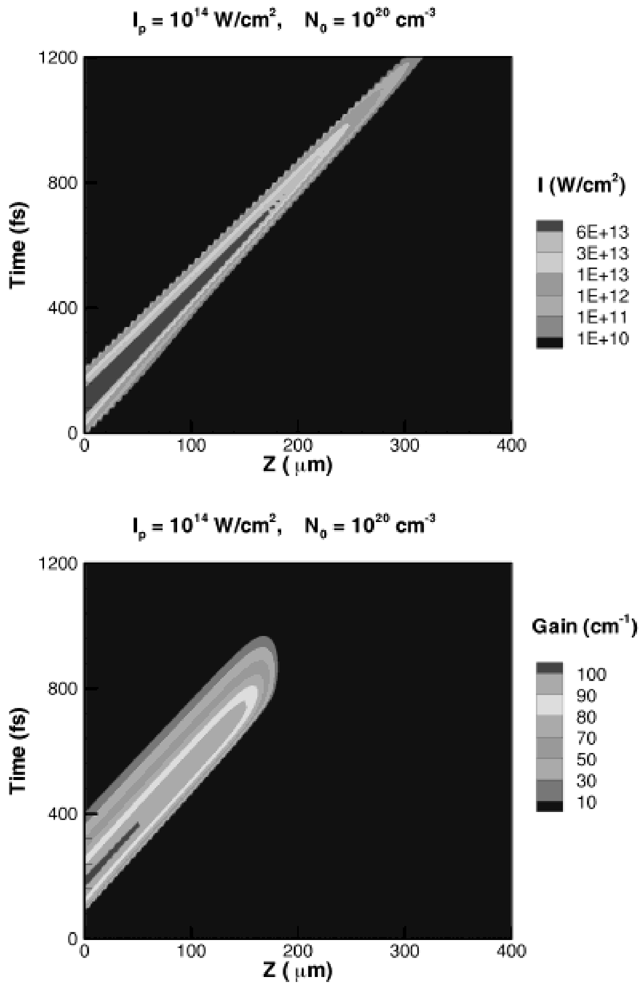

Fig. 5. Contour plot of pump intensity and gain for $N_0 = 10^{20}$ cm^{-3} and $I = 10^{14}$ W/cm^2. The pump pulse is seen to propagate only about 200 μm into the medium and, in spite of a gain coefficient of 100 cm^{-1}, the resulting gain length product is small.

part of the pulse is "eaten away" by the medium. Obviously a gain length product of 20 is easily achieved under this condition.

For comparison, in Figure 5 the case of a helium density of 10^{20} cm^{-3} is shown, again with a pump intensity of 10^{14} W/cm^2. Here the gain reaches a similar value (compare Fig. 3) but the pump does not propagate far into the medium. It is already absorbed after about 200 μm and thus the gain length product does not attain a high value. These diagrams show that the parameters of the medium have to be carefully chosen in order to realize a high gain length product.

4. SIMULATION RESULTS FOR HE II

This laser operates on the Lyman-α transition of hydrogenic helium with a wavelength of 30.4 nm. As stated in the introduction, first the pump must ionize atomic helium and then further ionize to bare nuclei. The first ionization results in an initial electron temperature of 20 eV (i.e., two thirds of

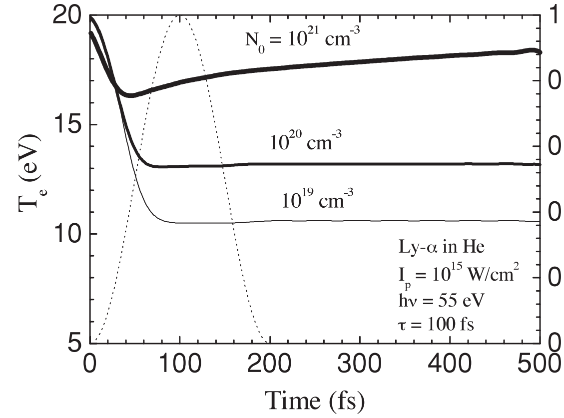

Fig. 6. Lyman-α laser in He II at 30.4 nm. Electron temperature for various densities as a function of time. Pump intensity is 10^{15} W/cm^2. Cooling of electrons by the second ionization is evident.

the excess energy of the 55 eV pump photon over the ionization potential). Only the second ionization generates very cold electrons. Figure 6 displays the temporal evolution of the electron temperature. The reduction of the electron temperature by the second step of ionization is clearly evident.

In Figure 7 the time-dependent gain coefficient for the He II Lyman-α transition at different densities is displayed. The pump intensity is 10^{15} W/cm^2, a factor of 10 higher than that used for He I. Here the gain rises very slowly for 10^{19} cm^{-3} and does not reach a high value. This is due to inefficient ionization of helium gas by the 55 eV photon. At higher densities the gain again reaches very high values.

By evaluating the gain at constant gas density and different peak pump intensities an interesting feature appears (see Fig. 8): The simulations exhibit an intensity window for the gain, that is, too low an intensity generates only low gain, but an intensity that is too high also results in small gain.

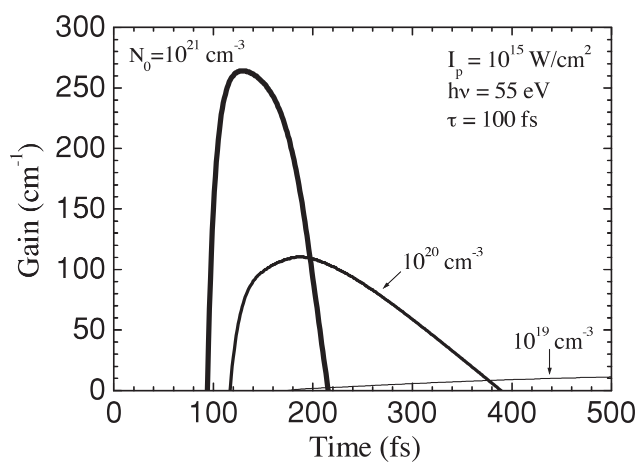

Fig. 7. Time-dependent gain coefficient for He II Lyman-α laser at 30.4 nm as for various densities. Pump intensity is 10^{15} W/cm^2.

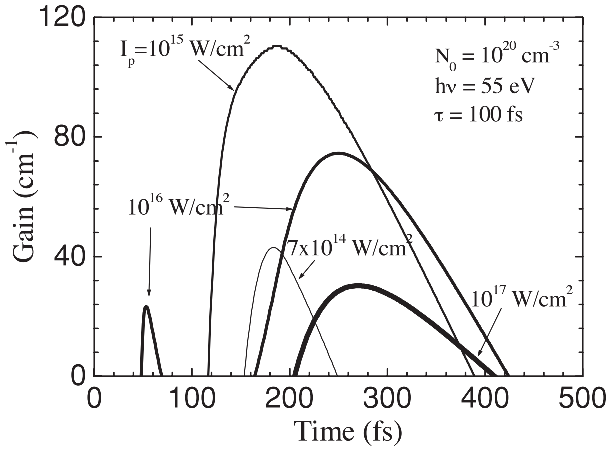

Fig. 8. Time-dependent gain coefficient for He II Lyman-α laser at a density of 10^{20} cm^{-3} for different pump intensities.

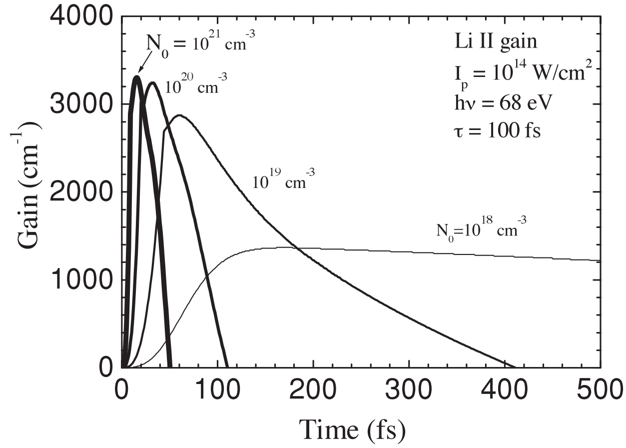

Fig. 9. Time-dependent gain coefficient of Li II inner-shell laser for a pump intensity of 10^{14} W/cm^2 at various densities.

This result seems surprising at first, but it can be understood by realizing that a high intensity leads to a high electron temperature by inverse bremsstrahlung heating. The gain is further reduced by ionization from the upper laser level.

5. LI II INNER-SHELL LASER

We present first simulation results for the case of an inner-shell laser (Duguay & Rentzepis, 1967) pumped by an XFEL. Interest in inner-shell lasers derives from the fact that the states forming the upper laser level are already occupied and, thus, very high gain should be generated. However, it had already been recognized in the first such proposal that inner-shell lasers suffer from a high rate of radiation-less loss of inversion due to the Auger effect.

The problem of the Auger transition is not pertinent if the atom contains only a single outer electron, as in Li and Na. In this case there is simply no electron for an Auger transition available. Although a number of papers have dealt with the Na laser, there is almost no literature on the similar laser in Li.

Ionization of a 1*s* electron of neutral lithium generates gain at the He-α line of Li II with a wavelength of 19.9 nm. Note however, that a transfer of the 2*s* electron of the neutral to the 2*p* level is required (Li *et al*., 1997). Data for the rate of such a transition in He-like ions are available for $Z > 5$ (Goett *et al*., 1980). These data indicate that the collision strength for intralevel mixing is very high. Nevertheless, at the lower densities the collisional rate may still not be high enough. A possibility for transferring population to the 2*p* level is to use a visible laser tuned to the 2*s*–2*p* resonance line of atomic lithium at $\lambda = 671$ nm. Figure 9 shows the result of a simulation of the gain on the He-α line of Li II for a pump intensity of 10^{14} W/ cm^2, pump photon energy of 67 eV, and at densities ranging from 10^{18} to 10^{21} cm^{-3}. Note that the pump photon energy is well above the Li *K*-edge of 54.7 eV. It was so chosen to generate relatively energetic electrons that would not immediately recombine. Such recombination would cause an effective broadening of the line. For these simulations the $n = 2$ levels of Li II were assumed to be occupied in accord with their statistical weights and thus rapid mixing of the 2*s* and 2*p* levels was supposed.

The figure shows that very high gain is indeed generated at 19.9 nm. The duration of the gain is limited by collisional ionization of the electron in the $n = 2$ level. At the (somewhat hypothetical) density of 10^{21} cm^{-3} the gain duration is 30 fs. This condition would thus lead to considerable shortening of the laser pulse compared with the pump pulse, a feature most welcome for many experiments. We finally note that this experiment will be quite challenging because a high lithium density is not easily achieved due to the low vapor pressure of that material.

6. PROSPECTS

We have shown that irradiation parameters accessible with the XFEL under construction at DESY generate high gain in atomic and hydrogenic helium and in helium-like lithium at wavelengths of 58.4 nm, 30.4 nm, and 19.9 nm, respectively. For the case of the He-α laser, in atomic helium a simulation of the propagation of the pump pulse was carried out and a high gain length product is predicted to be achievable. In view of these results, an experiment demonstrating a photopumped soft-X-ray laser appears to be feasible. We believe that such an experiment would result in increased knowledge of many aspects of photopumped X-ray lasers, such as the physics of photoionization and recombination, and give new information on the feasibility of simulations. Thus, the fields of atomic physics, plasma physics, and laser physics could take advantage of such an investigation. Of course, it would also be very exciting to scale this experiment to even shorter wavelengths using the hard X-rays expected from further developments of XFEL lasers.

ACKNOWLEDGMENTS

This work was supported in part by the Commission of the European Communities within the framework of the Euratom/Max-Planck-Institut für Plasmaphysik Association. Ke Lan's stay at Max-Planck-Institut für Quantenoptik is supported by an Alexander von Humboldt Fellowship.

REFERENCES

Bunkin, F.Y., Derzhiev, V.I. & Yakovlenko, S.I. (1981). Specifications for pumping x-ray laser with ionizing radiation. *Sov. J. Quantum Electron* **11**, 971–972.

Duguay, M.A. & Rentzepis, P.M. (1967). Some approaches to vacuum UV and X-ray lasers. *Appl. Phys. Lett.* **10**, 350–352.

Elton, R.C. (1990). *X-ray Lasers*. San Diego: Academic Press.

Gerth, C. (2001). *Free-electron laser at the TESLA Test Facility at DESY*. Soft X-ray Lasers and Applications IV, (E.E. Fill & J.J. Rocca eds.). San Diego, SPIE **4505**, 131–145.

Goett, S.J., Clark, R.E.H. & Sampson, D.H. (1980). Intermediate coupling collision strengths for $\Delta n = 0$ transitions produced by electron impact on highly charged He- and Be-like ions. *Atomic Data and Nucl. Data Tables* **25**, 185–217.

Goodwin, D.G. & Fill, E.E. (1988). Inversion and gain in hydrogenic ion levels induced by photoionization pumping. *J. Appl. Phys.* **64**, 1005–1014.

Goodwin, D.G. & Fill, E.E. (1990). Soft X-ray gain in hydrogenic ions: Line pumping, ionization pumping and transient excitation. *Appl. Phys. B* **50**, 177–185.

Griem, H.R. (1974). *Spectral line broadening by Plasmas*. New York and London: Academic Press.

Lan, K., Fill, E.E. & Meyer-ter-Vehn, J. (2003). Simulation of He-α and Lyman-α soft x-ray lasers in helium pumped by DESY/XFEL-ratiation. *Europhys. Lett.* **64**, 454–460.

Lan, K. & Zhang, Y. (2002). Theoretical studies of aluminum wire array Z-pinch implosions with varying masses and radii. *Eoru Phys. J. AP* **19**, 103–112.

Lan, K., Zhang, Y. & Zheng, W. (1999). Theoretical study on dischard-pumped soft x-ray laser in Ne-like Ar. *Phys. of Plasmas* **6**, 4343–4348.

Li, Y., Schillinger, J., Ziener, C. & Sauerberry, R. (1997). Reinvestigation of the Duguay soft X-ray laser: A new parameter space for high power femtosecond laser pumped systems. *Opt. Commun.* **144**, 118–124.

MacGowan, B.J., Da Silva, L.B., Fields, D.J., Keane, C.J., Koch, J.A., London, R.A., Matthews, D.L., Maxon, S., Mrowka, S., Osterheld, A.L., Scofield, J.H., Shimkaveg, G., Trebes, J.E. & Walling, R. (1992). Short wavelength x-ray laser research at the Lawrence Livermore National Laboratory. *Phys. Fluids B* **4**, 2326–2337.

Materlik, G. & Tschentscher, T. (2001). TESLA Technical Design Report, Part V, DESY, Hamburg.

Tallents, G.J. (2003). The physics of soft x-ray lasers pumped by electron collisions in laser plasmas. *J. Phys. D* **36**, R259–R276.